Decadal-Scale SST and Salinity Variations in the Central Tropical Pacific: Signatures of Natural and Anthropogenic Climate Change

INTAN S. NURHATI

School of Earth and Atmospheric Sciences, Georgia Institute of Technology, Atlanta, Georgia, and Center for Environmental Sensing and Modeling, Singapore–MIT Alliance for Research and Technology, Singapore

KIM M. COBB AND EMANUELE DI LORENZO

School of Earth and Atmospheric Sciences, Georgia Institute of Technology, Atlanta, Georgia

(Manuscript received 17 May 2010, in final form 3 December 2010)

ABSTRACT

Accurate projections of future temperature and precipitation patterns in many regions of the world depend on quantifying anthropogenic signatures in tropical Pacific climate against its rich background of natural variability. However, the detection of anthropogenic signatures in the region is hampered by the lack of continuous, century-long instrumental climate records. This study presents coral-based sea surface temperature (SST) and salinity proxy records from Palmyra Island in the central tropical Pacific over the twentieth century, based on coral strontium/calcium and the oxygen isotopic composition of seawater ($\delta^{18}O_{SW}$), respectively. On interannual time scales, the Sr/Ca-based SST record captures both eastern and central Pacific warming ''flavors'' of El Niño–Southern Oscillation (ENSO) variability ($R = 0.65$ and 0.67, respectively). On decadal time scales, the SST proxy record is highly correlated to the North Pacific gyre oscillation (NPGO) ($R = -0.85$), reflecting strong dynamical links between the central Pacific warming mode and extratropical decadal climate variability. Decadal-scale salinity variations implied by the coral-based $\delta^{18}O_{SW}$ record are significantly correlated with the Pacific decadal oscillation (PDO) ($R = 0.54$). The salinity proxy record is dominated by an unprecedented trend toward lighter $\delta^{18}O_{SW}$ values since the mid–twentieth century, implying that a significant freshening has taken place in the region, in line with climate model projections showing enhanced hydrological patterns under greenhouse forcing. Taken together, the new coral records suggest that low-frequency SST and salinity variations in the central tropical Pacific are controlled by different sets of dynamics and that recent hydrological trends in this region may be related to anthropogenic climate change.

1. Introduction

The detection of anthropogenic climate trends in the tropical Pacific is complicated by prominent interannual and decadal-scale natural climate variations in the region. Global temperature and precipitation patterns are heavily impacted by the interannual (2–7 yr) El Niño–Southern Oscillation (ENSO) phenomenon in the tropical Pacific, whose warm extremes are characterized by positive sea surface temperature and precipitation anomalies in the eastern and central tropical Pacific, along with a weakening of the zonal atmospheric Walker circulation (Rasmusson and Carpenter 1982). On decadal time scales, the Pacific decadal oscillation (PDO), defined as the leading mode of SST variability in the North Pacific (Mantua et al. 1997), is manifest as an ''ENSO like'' pattern of SST anomalies over the tropical Pacific (Zhang et al. 1997). Various mechanisms have been proposed to explain the PDO, most involving some combination of tropical and extratropical coupled ocean–atmosphere dynamics (e.g., Pierce 2002; Deser et al. 2004; Schneider and Cornuelle 2005). Of special significance to this manuscript, however, the PDO has been dynamically linked to ENSO variability via an ''atmospheric bridge'' (Alexander et al. 2002, 2004), whereby ENSO-related variations in the Aleutian low are integrated by the North Pacific Ocean to generate low-frequency PDO variability (Newman et al. 2003).

Corresponding author address: Intan Suci Nurhati, Center for Environmental Sensing and Modeling, Singapore–MIT Alliance for Research and Technology, S16-05-08, 3 Science Dr. 2, Singapore 117543.
E-mail: intan@smart.mit.edu

DOI: 10.1175/2011JCLI3852.1

© 2011 American Meteorological Society

Analyses of instrumental SST in the Pacific also identify a tropical Pacific climate pattern characterized by central Pacific warming (CPW) flanked by cooler SSTs in the eastern and western tropical Pacific (Weare et al. 1976; Latif et al. 1997; Trenberth and Stepaniak 2001; Larkin and Harrison 2005; Ashok et al. 2007; Kug et al. 2009; Kao and Yu 2009). The interannual expression of the CPW pattern is often referred to as ENSO Modoki or ''pseudo ENSO'' (Ashok et al. 2007), referring to the lack of SST warming in the eastern tropical Pacific that characterizes canonical ENSO events. Different SST distributions translate into markedly different atmospheric teleconnections associated with the ENSO Modoki versus the canonical ENSO (Kumar et al. 2006; Wang and Hendon 2007; Weng et al. 2009). ENSO Modoki has also been associated with increased tropical cyclone frequency in the Pacific and Atlantic basins (Kim et al. 2009; Chen and Tam 2010). On decadal time scales, the CPW pattern has been dynamically linked to the North Pacific gyre oscillation (NPGO) (Di Lorenzo et al. 2008), which represents the second leading mode of SST variability in the North Pacific, after the PDO. Much as canonical ENSO is linked to the PDO through variations in the Aleutian low, interannual-scale CPW variations have been dynamically linked to the NPGO through variations in the atmospheric North Pacific Oscillation (Di Lorenzo et al. 2010).

Significant natural climate variability in the tropical Pacific, when combined with large uncertainties in early twentieth-century instrumental climate data from this region (e.g., Deser et al. 2010), complicate the detection of anthropogenic climate trends in this region. A majority of coupled global climate models (GCMs) in the Fourth Assessment Report of the Intergovernmental Panel on Climate Change (AR4 IPCC) project a trend toward a weakened tropical Pacific zonal SST gradients under continued anthropogenic forcing (Meehl et al. 2007), in line with analyses of some instrumental climate datasets (Vecchi et al. 2006; Bunge and Clarke 2009). However, Vecchi et al. (2008) highlight large uncertainties in instrumental SST datasets that contain tropical Pacific SST trends of opposing signs. Recent analyses of GCM output suggest that anthropogenic warming may be concentrated in the central tropical Pacific (Xie et al. 2010) and along the equator (Liu et al. 2006; DiNezio et al. 2009), perhaps related to a shift toward ENSO Modoki under anthropogenic forcing (Yeh et al. 2009). Such changes in regional SST warming, as projected in climate models, would have a profound effect on the pattern of global precipitation changes in the twenty-first century (Xie et al. 2010). Under uniform warming, the Clausius–Clapeyron relationship predicts enhanced global hydrological patterns where wet regions are getting wetter and vice versa (Held and Soden 2006), but long-term precipitation trends are difficult to extract from relatively short instrumental precipitation datasets. Century-long, continuous proxy records from key locations in the tropical Pacific are required to identify potential anthropogenic trends in SST and hydrology against a rich background of interannual to decadal-scale natural climate variability in the tropical Pacific.

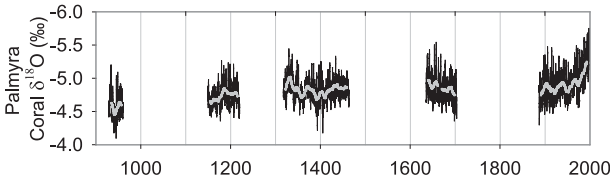

FIG. 1. Modern and fossil coral δ^{18}O records from Palmyra Island (6°N, 162°W) spanning the last millennium. A late-twentieth-century trend toward lower coral δ^{18}O values is indicative of recent warming and/or freshening in the central tropical Pacific (modified after Cobb et al. 2003).

Monthly resolved coral geochemical records that provide well-calibrated reconstructions of SST and/or hydrological variability have been used to investigate natural and anthropogenic climate variability over the last several centuries [see reviews by Gagan et al. (2000) and Corrège (2006)]. The oxygen isotopic composition (δ^{18}O) of coral skeletal aragonite reflects changes in SST as well as changes in the δ^{18}O of seawater ($\delta^{18}O_{SW}$), the latter linearly related to seawater salinity (Fairbanks et al. 1997). In the tropical Pacific, coral δ^{18}O records have been used to reconstruct preinstrumental ENSO variability (Cole et al. 1993; Tudhope et al. 2001; Evans et al. 2002; Cobb et al. 2003), decadal-scale tropical Pacific climate variability (Cobb et al. 2001; Ault et al. 2009), and tropical Pacific climate trends (Urban et al. 2000; Nurhati et al. 2009). When combined with measurements of coral Sr/Ca ratios as a proxy for SST (Beck et al. 1992; Alibert and McCulloch 1997), coral δ^{18}O can be used to reconstruct changes in $\delta^{18}O_{SW}$ as a proxy for salinity (McCulloch et al. 1994; Gagan et al. 1998; Hendy et al. 2002; Kilbourne et al. 2004; Linsley et al. 2006). To date, no long coral Sr/Ca or $\delta^{18}O_{SW}$ records have been generated from the central tropical Pacific, despite the fact that models have identified this region as the locus for large anthropogenic trends in SST and hydrology.

This study presents monthly resolved, century-long reconstructions of central tropical Pacific SST and salinity based on coral Sr/Ca and $\delta^{18}O_{SW}$, respectively, from Palmyra Island (6°N, 162°W). A previously published millennium-long compilation of living and fossil coral δ^{18}O records from Palmyra is characterized by a late-twentieth-century trend toward negative coral δ^{18}O values (Fig. 1) (Cobb et al. 2003), suggesting warming

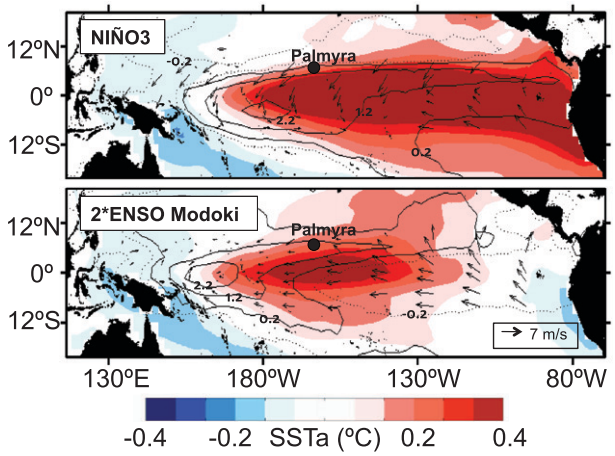

FIG. 2. SST anomalies (°C, colors), precipitation anomalies (mm day^{-1}, contours), and mean wind stress (m s^{-1}, arrows) associated with (top) eastern and (bottom) central Pacific ENSO variability. (top) SST and precipitation anomalies regressed on the Niño-3 SST anomaly. Mean wind stress are shown during the peak months (December–February) of the 1982/83 and 1997/98 El Niño events (Niño-3 SST anomaly >2°C). (bottom) SST and precipitation anomalies regressed on the ENSO Modoki index, then multiplied by 2. Mean wind stress during the peak months (July–September) of the 1994 and 2004 El Niño events (ENSO Modoki index SST anomaly >2°C). SST data are from Reynolds et al. (2002), precipitation data are from Xie and Arkin (1997), and wind stress data are from the Tropical Ocean Atmosphere buoys [information online at http://www.pmel.noaa.gov/tao/; see also McPhaden et al. (1998)].

and/or freshening conditions. That this negative coral δ^{18}O trend is unprecedented in the last millennium strongly suggests that anthropogenic climate forcing has caused appreciable warming and/or freshening in this region, in line with results from other central tropical Pacific coral δ^{18}O records (Evans et al. 1999; Urban et al. 2000). The new Palmyra Sr/Ca-derived SST and $\delta^{18}O_{SW}$-based salinity proxy records presented in this study allow us to quantify the warming and freshening contributions to the unprecedented late-twentieth-century Palmyra coral δ^{18}O trend, providing a much-needed test of GCM anthropogenic climate projections in this key region.

2. Methodology

a. Study site

Palmyra Island (6°N, 162°W), located in the Line Islands chain in the central tropical Pacific, is heavily influenced by ENSO variability (Fig. 2). During El Niño warm events, SST anomalies of roughly +0.2°C are accompanied by positive precipitation anomalies of approximately +1 mm day^{-1} at the study site (Fig. 2, top). During El Niño Modoki warm events, warming is concentrated in the central tropical Pacific, with positive precipitation anomalies displaced westward toward the date line (Fig. 2, bottom). Note that, as the SST and precipitation impacts of ENSO Modoki at Palmyra are roughly half as large as the impacts associated with canonical El Niño events, the ENSO Modoki index is multiplied by two for the analyses presented in this paper. There are profound differences in large-scale atmospheric circulation associated with the canonical and Modoki ENSOs, as documented by Weng et al. (2009). Canonical El Niño events result in weaker tropical Pacific trade winds, bringing warmer and fresher conditions to the central tropical Pacific. Strong central tropical Pacific warming associated with El Niño Modoki events drives low-level convergence, maintaining easterly trade winds across the eastern tropical Pacific that drive the upwelling of relatively cool, saline waters to the east of Palmyra. The Palmyra coral-based Sr/Ca-derived SST and $\delta^{18}O_{SW}$-based salinity proxy data presented in this study are available via the NOAA Paleoclimatology World Data Center Web site (ftp://ftp.ncdc.noaa.gov/pub/data/paleo/coral/east_pacific/palmyra2011.txt).

b. Coral Sr/Ca measurements

The *Porites* coral core analyzed for this study was collected in May 1998, and the associated 112-yr-long δ^{18}O record and chronology were presented in Cobb et al. (2001). Sampling for coral Sr/Ca was conducted adjacent to the original δ^{18}O sampling transect at the same 1-mm increments used for δ^{18}O sampling, guaranteeing a point-by-point correspondence between the original coral δ^{18}O time series and the new coral Sr/Ca time series. Coral Sr/Ca ratios were measured using a Jobin Yvon (JY) Ultima 2C inductively coupled plasma optical emission spectroscope (ICP-OES) with analytical precision less than ±0.07% or ±0.006 mmol mol^{-1}(1σ) using the Schrag (1999) nearest-neighbor correction method. Details on intra- and intercolony coral δ^{18}O and Sr/Ca reproducibility of Line Island corals are presented in the supplementary information of Nurhati et al. (2009).

c. Reconstructing SST and salinity proxy records

The new Palmyra coral Sr/Ca record was transformed into SST by calibrating the coral Sr/Ca time series against 1° × 1° Intergovernmental Oceanographic Commission/World Meteorological Organization Integrated Global Ocean Services System (IGOSS) SST data over the period 1982–98 (Reynolds et al. 2002). The equation for the Sr/Ca–SST calibration via reduced major axis (RMA) regression is as follows:

$$\mathrm{SST} = 130.43 - 11.39 \times \mathrm{Sr/Ca}$$
$$(R = -0.71, \quad N_{\mathrm{eff}} = 28, \quad \mathrm{CI} > 95\%). \qquad (1)$$

The selection of the Reynolds et al. (2002) SST dataset as a calibration target is motivated by its similarity to an in situ SST record from Palmyra [see supplementary information of Nurhati et al. (2009)]. The intercept and slope of the Sr/Ca–SST calibration at Palmyra fall within the range of existing Sr/Ca–SST relationships for *Porites* corals (Corrège 2006 and references therein). In comparing the Palmyra coral Sr/Ca–SST calibration to other published calibrations, it is important to note that most published coral Sr/Ca–SST calibrations use ordinary least squares (OLS) regression: the Palmyra OLS regression yields a calibration of -0.06 mmol °C^{-1}, well within the -0.04 to -0.08 mmol °C^{-1} published range for *Porites* corals. The RMA regression technique used in this study represents an improvement over the OLS regression typically utilized in coral–SST calibrations, as it minimizes residuals in two variables that both have nonzero uncertainties, providing more robust and accurate paleoSST estimates (Solow and Huppert 2004). Significance tests for correlation coefficients reported throughout this paper are based on a Student's t test after calculating effective degrees of freedom (N_{eff}), which accounts for lag-one serial autocorrelation in the two time series as outlined by Bretherton et al. (1999).

The estimation of uncertainty in the coral Sr/Ca-based SST proxy reconstruction takes into account contributions of uncertainties from the analytical precision of Sr/Ca measurements and the Sr/Ca–SST calibration. Analytical uncertainty accounts for ±0.07°C (1σ), and the uncertainty associated with the intercept and slope of the SST–Sr/Ca relationship translates into a large error of ±7.85°C (1σ) ($\sigma \equiv$ standard deviation). Taken together, the compounded error bar for the reconstructed SST record is conservatively reported as ±7.85°C (1σ) via an additive error propagation, highlighting that the uncertainties in the Sr/Ca–SST calibration dominate the total error (see the appendix). It is important to note that this large error is associated with the calculation of absolute SST only. Relative changes in SST, upon which the results of this study are based, are associated with a much smaller error of ±0.10°C (1σ) (see the appendix). In other words, large uncertainties in the slope and intercept of the Sr/Ca–SST relationship do not change the character of the coral-based SST nor the $\delta^{18}O_{SW}$ reconstructions.

Changes in $\delta^{18}O_{SW}$ as a proxy for salinity were reconstructed by subtracting the Sr/Ca-derived SST contribution from the coral $\delta^{18}O$ record following the method outlined in Ren et al. (2003), where the residual is the $\delta^{18}O_{SW}$. The relevant equations are as follows:

$$\Delta\delta^{18}O_{\mathrm{CORAL}} = \Delta\delta^{18}O_{\mathrm{SST}} + \Delta\delta^{18}O_{\mathrm{SW}} \qquad (2)$$

and

$$\Delta\delta^{18}O_{\mathrm{SST}} = \left[\overline{\Delta\mathrm{SrCa}}\,\frac{\partial \mathrm{SST}}{\partial \mathrm{SrCa}}\,\frac{\partial\delta^{18}O_{\mathrm{CORAL}}}{\partial \mathrm{SST}}\right]. \qquad (3)$$

We use an empirically derived $\partial\delta^{18}O_{\mathrm{CORAL}}/\partial$SST value of -0.21 ± 0.03‰°C^{-1} (Ren et al. 2003). We derive the $\delta^{18}O_{SW}$ time series by integrating $\Delta\delta^{18}O_{SW}$ values at each time step, beginning with $\delta^{18}O_{SW}$ values of 0.39‰ estimated by transforming Palmyra climatological sea surface salinity (Levitus et al. 1994) into average $\delta^{18}O_{SW}$ values using an empirical $\delta^{18}O_{SW}$–salinity relationship for the central tropical Pacific (Fairbanks et al. 1997). The absolute $\delta^{18}O_{SW}$ values may be inaccurate, but the relative changes in $\delta^{18}O_{SW}$ are unaffected by the choice of absolute $\delta^{18}O_{SW}$. The compounded error bar for the $\delta^{18}O_{SW}$ record is conservatively reported as ±0.1‰ (1σ), which takes into account uncertainties in analytical measurements of coral $\delta^{18}O$ and Sr/Ca, SST–Sr/Ca calibration, and coral $\delta^{18}O$ regression (see appendix).

d. Assessment of diagenesis

Given that even minor diagenesis is associated with higher coral Sr/Ca values (cooler SST bias) in a suite of modern corals (Enmar et al. 2000; Quinn and Taylor 2006; Hendy et al. 2007), the skeletal surfaces of the Palmyra modern coral were examined by a scanning electron microscope (SEM). SEM images were obtained using a Hitachi S-800 Field Gun Emission SEM and a 126 LEO 1530 Thermally assisted Field Emission SEM. Coral fragments were sampled in the 1886, 1905, 1917, 1922, 1927, 1939, 1949, and 1971 horizons of the core. SEM sampling horizons were concentrated toward the bottom of the core, where diagenesis is more likely to occur (Enmar et al. 2000), and at core depths characterized by relatively high Sr/Ca values (''cool'' reconstructed SST) (Fig. 3). The SEM images reveal secondary aragonite needles coating the 1886 horizon of the core (Figs. 3a and 3b). These ~2-μm-long aragonite needles are very small in comparison to the 20-μm-long needles that are documented in diagenetically compromised sections of other modern corals (Hendy et al. 2007; Nurhati et al. 2009), so we infer that they had little impact on the coral Sr/Ca record. The only other SEM photos that revealed any signs of diagenesis are associated with the 1917 horizon of the core, which is characterized by a thin, smooth coating of unidentified mineralogy (Fig. 3d). Relatively high coral Sr/Ca values (inferred cooling) measured in the 1917 horizon of the core (Fig. 4b) may

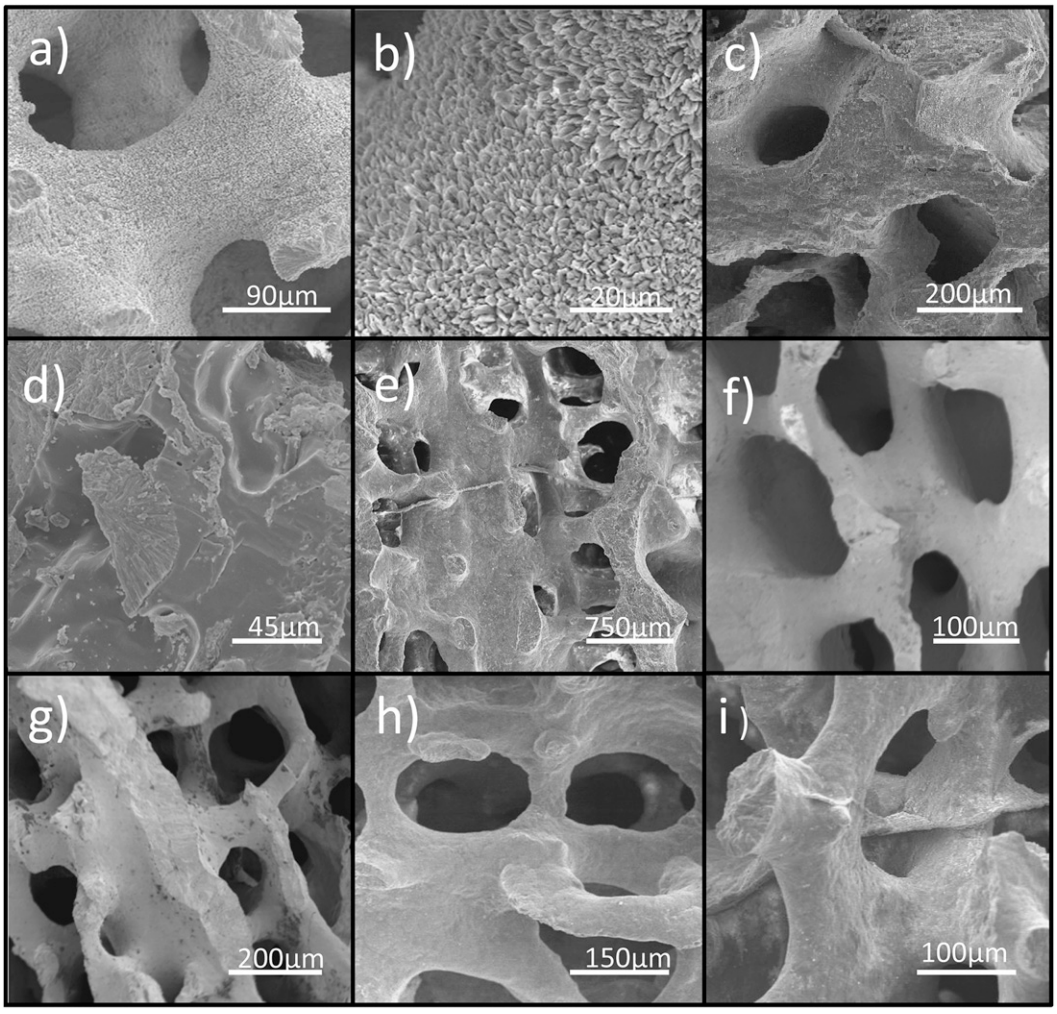

FIG. 3. SEM images of the Palmyra modern coral from the (a),(b) 1886, (c) 1905, (d) 1917, (e) 1922, (f) 1927, (g) 1936, (h) 1949, and (i) 1971 horizons.

be related to these coatings. However, reanalysis extended reconstruction SST (ERSST) data from the Palmyra grid point document significant cooling in 1917, making it difficult to determine if the observed diagenesis impacted coral Sr/Ca values. While the downcore extent of the 1917-related coatings is poorly constrained, SEM photos from the 1905 and 1922 horizons of the core show no signs of diagenesis. Therefore, with the possible exception of the 1917 horizon and near vicinity, the new 112-yr-long coral Sr/Ca record presented here appears to be unaffected by diagenesis.

3. Results and discussion

The previously published Palmyra coral $\delta^{18}O$ record reflects a combination of SST and $\delta^{18}O_{SW}$ variability, and is characterized by strong interannual and decadal-scale variability, as well as a prominent trend toward lower coral $\delta^{18}O$ values beginning in the mid-1970s (Cobb et al. 2001; Fig. 4a). The trend, which amounts to roughly $-0.5‰$ over the course of two decades, implies a trend toward warmer and/or wetter conditions in the central tropical Pacific, and is unprecedented in a millennium-long compilation of fossil coral $\delta^{18}O$ records from Palmyra (Cobb et al. 2003; Fig. 1).

The new coral Sr/Ca-derived SST proxy record exhibits interannual and decadal variability of roughly $\pm 1°C$ (Fig. 4b). There is a late-twentieth-century warming trend, but it is not statistically significant given the strong interannual and decadal-scale variability contained in the SST proxy record. Overall, the coral-derived SST proxy record shows good agreement with the reanalysis ERSST (Smith et al. 2008) from the Palmyra grid point ($R = 0.60$ for raw monthly data), with similarly

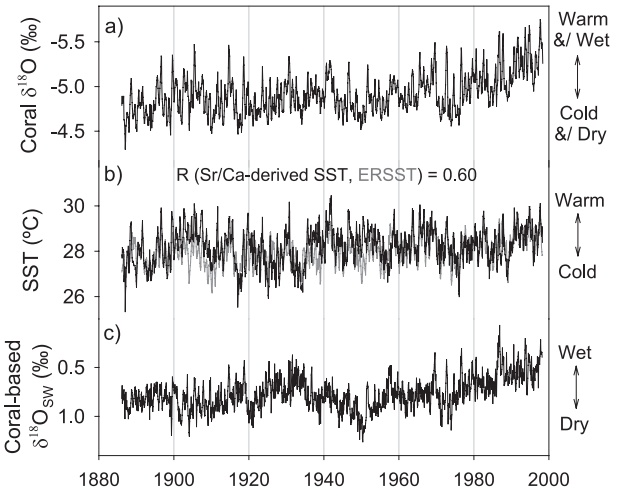

FIG. 4. Palmyra coral monthly resolved $\delta^{18}O$, Sr/Ca-derived SST, and $\delta^{18}O_{SW}$ records from 1886 to 1998. (a) Palmyra coral $\delta^{18}O$ record (Cobb et al. 2001), (b) Sr/Ca-derived SST (black) plotted with ERSST (gray; Smith et al. 2008), and (c) $\delta^{18}O_{SW}$-based salinity record.

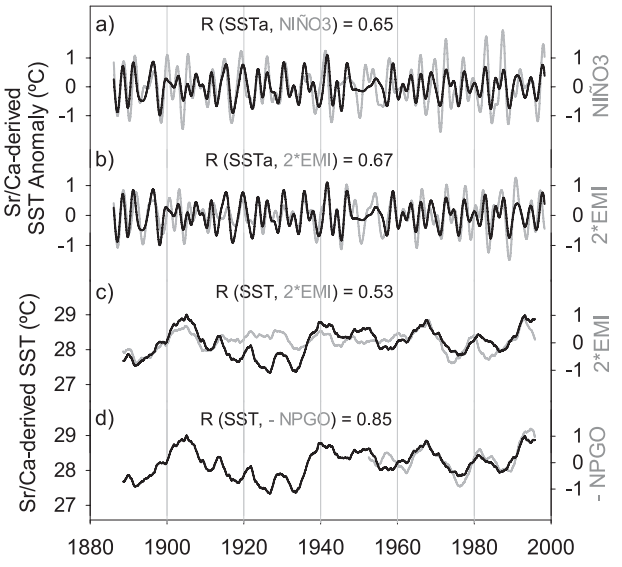

FIG. 5. Interannual and decadal-scale coral Sr/Ca-derived SST variability at Palmyra plotted with tropical Pacific instrumental climate indices: (a) interannual (2–7-yr bandpassed) Sr/Ca-derived SST anomalies (black) and Niño-3 SST anomalies (gray), (b) interannual (2–7-yr bandpasssed) Sr/Ca-derived SST anomalies (black) and the 2×ENSO Modoki index (gray), and (c) decadal-scale Sr/Ca-derived SST (black) and 2×ENSO Modoki index (gray) plotted as 5-yr running averages. (b) Decadal-scale Sr/Ca-derived SST (black) and –NPGO index (gray) plotted as 5-yr running averages. All correlations are statistically significant at a 95% confidence level using a Student's *t* test and adjusting for serial autocorrelation.

high correlations for interannual ($R = 0.72$ for 2–7-yr bandpassed) and decadal-scale ($R = 0.61$ for 8-yr lowpassed) versions of the records.

The Palmyra coral $\delta^{18}O_{SW}$ record is dominated by decadal-scale variability and a relatively large freshening trend over the late twentieth century (Fig. 4c). A visual comparison of the three coral records plotted in Fig. 4 reveals that the $\delta^{18}O_{SW}$ trend is responsible for the large trend in coral $\delta^{18}O$, with warming playing a secondary role. The marked differences between the coral Sr/Ca-derived SST and the $\delta^{18}O_{SW}$-based salinity proxy records are striking, implying that low frequency SST and salinity variations are governed by different dynamics. The remainder of this paper investigates the large-scale climate controls on Palmyra SST and salinity on interannual, decadal, and secular time scales.

a. Interannual to decadal-scale tropical Pacific climate variability

1) CORAL Sr/Ca-DERIVED SST VARIABILITY

On interannual (2–7 yr) time scales, the SST proxy record captures ENSO variability in the central tropical Pacific, as reflected by significant correlations with the central tropical Pacific Niño-3.4 SST index [SST anomalies averaged over 5°N–5°S, 120°–170°W (Kaplan et al. 1998)] ($R = 0.71$, 1886–1998, $N_{eff} = 32$, CI > 95%). High correlations with SST anomalies in the Niño-3 region [5°N–5°S, 90°–150°W(Kaplan et al. 1998)] ($R = 0.65$, 1886–1998, $N_{eff} = 33$, CI > 95%), see Fig. 5a, as well as high correlations with the ENSO Modoki index of Ashok et al. (2007) ($R = 0.67$, 1886–1998, $N_{eff} = 34$, CI > 95%), see Fig. 5b, reflect the sensitivity of the Palmyra coral Sr/Ca record to both eastern and central Pacific "flavors" of ENSO variability, respectively. These significant correlations reflect the fact that warm SST anomalies occur in the central tropical Pacific during both canonical El Niño events as well as El Niño Modoki events, and vice versa during La Niña cool events.

On decadal time scales, the SST proxy record is highly correlated to low frequency variability associated with the CPW, as evidenced by significant correlations between the 5-yr running-average versions of the SST proxy record and the ENSO Modoki index ($R = 0.53$, 1888–1995, $N_{eff} = 17$, CI > 95%), see Fig. 5c. The SST proxy record is significantly correlated with the 5-yr-averaged NPGO index (Di Lorenzo et al. 2008) ($R = -0.85$, 1952–95, $N_{eff} = 10$, CI > 95%), see Fig. 5d, reflecting strong dynamical linkages between central tropical Pacific SST and the decadal-scale NPGO, as uncovered by Di Lorenzo et al. (2010). Over the same period, the correlation between the SST proxy record and the ENSO Modoki index is similarly high ($R = 0.76$, 1952–95, $N_{eff} = 8$, CI > 95%). Statistically significant correlations between the coral Sr/Ca-derived SST proxy

record, the ENSO Modoki index, and the NPGO are also found when comparing 8-yr low-passed versions of the records. The SST proxy record is not significantly correlated to the PDO index ($R = -0.03$, 1902–95), which is somewhat surprising given that the PDO is understood as the decadal expression of ENSO-related variability in the North Pacific (Alexander et al. 2002). This suggests that low-frequency central Pacific SST variations are more closely related to the NPGO than the PDO and, furthermore, likely play an important role in shaping the temporal evolution of the NPGO.

Regressions of the NPGO and the PDO with Pacific basin instrumental SST data reveal that the amplitude of low-frequency central tropical Pacific SST anomalies associated with the NPGO are almost twice as large as those associated with the PDO (Fig. 6). Both North Pacific decadal-scale climate modes are associated with a similar spatial pattern characterized by warming that extends from the central tropical Pacific to the northeast Pacific, with maximum cool anomalies in the central North Pacific. However, at Palmyra, the SST anomalies associated with low frequency variations in the NPGO are ±0.15°C, compared to ±0.05°C for low frequency variations of the PDO. Therefore, it is not surprising that the coral Sr/Ca-derived SST proxy record is more sensitive to the NPGO variations, given Palmyra's location in the central tropical Pacific. The decadal-scale variability captured in the Palmyra Sr/Ca-derived SST proxy record is consistent with the previous analyses of instrumental and proxy climate records from the tropical Pacific. First, wavelet analysis of instrumental SST data from the central tropical Pacific reveals decadal variability with a ~12–13-yr periodicity (Kug et al. 2009), similar to that associated with the NPGO, but significantly shorter than the PDO's multidecadal variability. Strong decadal variability with 12–13-yr power was also uncovered in analyses of the original Palmyra coral $\delta^{18}O$ record (Cobb et al. 2001) and in analyses using multiple coral $\delta^{18}O$ records from across the tropical Pacific (Holland et al. 2007; Ault et al. 2009). Taken together, these results lend further support to the idea that the central tropical Pacific is characterized by appreciable decadal-scale SST variability.

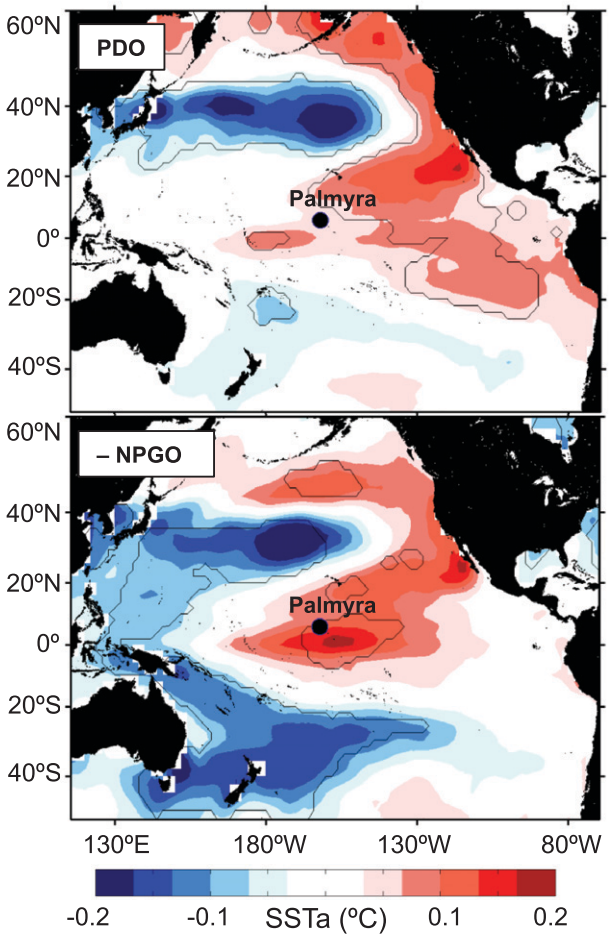

FIG. 6. Regressions of Pacific SST anomalies with two indices of Pacific decadal-scale climate variability: SST regressed against an 8-yr low-passed (top) PDO index (Mantua et al. 1997) from 1900 to 2009 and (bottom) −NPGO index (Di Lorenzo et al. 2008) from 1950 to 2009. Contour lines indicate areas where correlation coefficients (not plotted) exceed the 95% significance level, using a Student's *t* test and adjusting for serial autocorrelation. SST data are from Reynolds et al. (2002).

2) $\delta^{18}O_{SW}$-BASED SALINITY VARIABILITY

On interannual (2–7-yr bandpassed) time scales, the Palmyra coral-based $\delta^{18}O_{SW}$ record is significantly correlated to eastern Pacific ENSO variability ($R = -0.49$ with the Niño-3 index, 1886–1998, $N_{eff} = 41$, CI > 95%; see Fig. 7a), but is weakly correlated to central Pacific ENSO variability ($R = -0.19$). To understand the coral-based $\delta^{18}O_{SW}$ record's sensitivity to eastern Pacific ENSO variability and its poor sensitivity to central Pacific ENSO variability, it is necessary to consider the various influences—both atmospheric and oceanographic—that determine seawater $\delta^{18}O$ at Palmyra. Changes in the precipitation minus evaporation balance in the central tropical Pacific, as well as changes in the advection (whether vertical or horizontal) of high and low salinity seawater to the site, would have effects on seawater $\delta^{18}O$ at Palmyra. As previously documented in coral-based $\delta^{18}O_{SW}$ records (Gagan et al. 2000; Kilbourne et al. 2004; Linsley et al. 2006), precipitation strongly influences surface seawater $\delta^{18}O$ because tropical Pacific rainwater is generally depleted in $\delta^{18}O$ relative to the surface ocean (Cole and Fairbanks 1990). Figure 2 illustrates that positive precipitation anomalies occur at

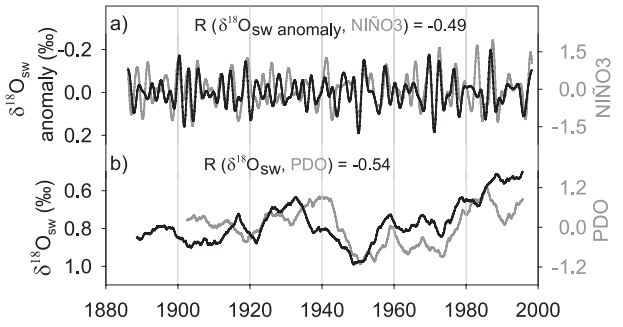

FIG. 7. Interannual and decadal-scale variability of the Palmyra coral $\delta^{18}O_{SW}$ record plotted with Pacific instrumental climate indices: (a) interannual (2–7-yr bandpassed) $\delta^{18}O_{SW}$ anomalies (black) and Niño-3 SST anomalies (gray) and (b) decadal-scale $\delta^{18}O_{SW}$ (black) and the PDO (gray) variability, plotted as 5-yr running averages. All correlations are statistically significant at a 95% confidence level using a Student's t test and adjusting for serial autocorrelation.

Palmyra during both flavors of ENSO but that, during central Pacific warm events, the locus of maximum precipitation is shifted far west of Palmyra, with negative precipitation anomalies along the equator from 80° to 160°W. Therefore, the observed precipitation patterns are consistent with the coral $\delta^{18}O_{SW}$ record's high (low) sensitivity to eastern (central) tropical Pacific ENSO activity.

ENSO is also characterized by profound changes in horizontal and vertical advection in the vicinity of Palmyra that likely contribute to interannual variability in the coral $\delta^{18}O_{SW}$ record. Both instrumental and numerical modeling studies support an eastward extension of the low salinity, low $\delta^{18}O_{SW}$ western Pacific fresh pool during strong El Niño events (Picaut et al. 1996; Delcroix and Picaut 1998), although these studies do not distinguish between the two flavors of ENSO. With respect to vertical advection, strong easterly winds across the cold tongue region during central Pacific warm events (Fig. 2b) will drive wind-driven upwelling, bringing relatively saline waters from subsurface to the surface in the central tropical Pacific (Wyrtki 1981). Such upwelling is virtually shut off during eastern Pacific warm events when trade winds significantly weaken (Fig. 2a). We conclude that marked differences in large-scale patterns of precipitation and ocean advection during eastern versus central Pacific warm events explain why eastern Pacific warm events are well recorded in $\delta^{18}O_{SW}$ at Palmyra, while central Pacific warm events are not.

Echoing the dominance of eastern Pacific ENSO on interannual variability in $\delta^{18}O_{SW}$, large decadal-scale variations in the $\delta^{18}O_{SW}$-based salinity proxy record are closely related to the PDO, but poorly correlated to both central Pacific warming and the NPGO. The correlation between 5-yr running-average versions of the $\delta^{18}O_{SW}$ record and the PDO is −0.54 (1902–95, $N_{eff} = 29$, CI > 95%; Fig. 7b), versus statistically insignificant correlations of −0.04 and 0.27 computed with ENSO Modoki (1902–95) and the NPGO (1952–95), respectively. The $\delta^{18}O_{SW}$ record implies that significant seawater freshening occurs during PDO warm regimes (1925–46 and 1977–98), with more saline conditions during the PDO cold regime (1947–75) (Mantua et al. 1997). The strong correlation between the $\delta^{18}O_{SW}$ record and the PDO implies that the PDO impacts salinity in the central tropical Pacific, as hypothesized based on analysis of instrumental salinity data available in the late twentieth century (Delcroix et al. 2007).

The new coral records reveal that central tropical Pacific seawater $\delta^{18}O$ variations track canonical eastern Pacific ENSO and the PDO, with poor correlations to central Pacific warming and the NPGO. However, the strong parallels between interannual and decadal-scale $\delta^{18}O_{SW}$ variability uncovered in this study do not provide any mechanistic insights into the causes of $\delta^{18}O_{SW}$ (or salinity) variability on decadal time scales. Delcroix et al. (2007) shows that PDO-related changes in salinity, precipitation, and wind-driven advection in the tropical Pacific are remarkably similar to those observed with eastern Pacific ENSO variability. But it is important to keep in mind that whereas interannual $\delta^{18}O_{SW}$ variations can largely be explained by months-long changes in precipitation minus evaporation and zonal advection, decadal-scale $\delta^{18}O_{SW}$ variations must be maintained in the face of effective ocean mixing that occurs on decadal time scales. Ultimately, given the dearth of salinity data from the tropical Pacific, the atmospheric and the oceanographic contributions to decadal-scale changes in salinity across the tropical Pacific could be investigated in existing coupled GCM simulations, as the Palmyra $\delta^{18}O_{SW}$ record suggests that such changes are relatively large.

b. Secular changes in tropical Pacific climate variability

Having established that the Palmyra coral Sr/Ca-derived SST and $\delta^{18}O_{SW}$-based salinity proxy records are robust indicators of tropical Pacific climate change on interannual to multidecadal time scales, these records can be used to assess the SST versus salinity contributions to the late-twentieth-century trend in coral $\delta^{18}O$ that is unprecedented in the last millennium (Cobb et al. 2003). If the millennium-long coral $\delta^{18}O$ record represents an accurate depiction of centuries-long climate variability in the central tropical Pacific, then the late-twentieth-century trend in coral $\delta^{18}O$ is likely related to anthropogenic climate change, and it is important to assess whether it is driven by warming and/or freshening.

1) CORAL Sr/Ca-DERIVED SST TREND

The coral Sr/Ca-derived SST proxy record is characterized by a +0.53 ± 0.10°C (1σ) linear warming trend that is relatively uniform throughout the last century (1886–1998; see appendix for explanation of the trend error estimate). However, strong decadal variability throughout the coral SST proxy record means that the SST trend is only significant at a 75% confidence level (as assessed with a Monte Carlo autoregressive significance test using $N = 3000$; see appendix for explanation of trend error estimation). Nonetheless, the coral's inferred warming trend is roughly equivalent to the observed +0.6°C increase in global SST over the twentieth century (Solomon et al. 2007) and falls well within the range of instrumental SST trends at Palmyra derived from various gridded SST datasets [Fig. 8; +0.36°C for Hadley (Rayner et al. 2006), +0.48°C for Kaplan (Kaplan et al. 1998), and +0.74°C for ERSST (Smith et al. 2008)] over the same period. The discrepancies among the instrumental SST datasets are likely associated with different strategies for bias correction and interpolation (Reynolds et al. 2007). However, while the size of the coral-based SST trend falls within the range of instrumental SST trends, the coral SST proxy record is characterized by decadal-scale variations in the early twentieth century that are not reflected in any of the instrumental SST datasets. Ultimately, resolving the magnitude and character of early twentieth-century decadal-scale SST variations in the central tropical Pacific requires the improvement of existing SST databases, likely combined with the generation of additional paleoSST records from this region.

2) $\delta^{18}O_{SW}$-BASED SALINITY TREND

The coral-based $\delta^{18}O_{SW}$ salinity proxy record exhibits a strong freshening trend beginning in the mid–twentieth century. The century-long $\delta^{18}O_{SW}$ trend of $-0.25 \pm 0.06‰$ (1σ) is statistically significant at a 99% confidence level (as assessed with a Monte Carlo autoregressive significance test using $N = 3000$; see appendix for an explanation of trend error estimation). The inferred freshening is consistent with enhanced global hydrological patterns (Held and Soden 2006) and a weakened tropical atmospheric circulation under global warming (Vecchi et al. 2006). If weakened trade winds under anthropogenic forcing lead to an eastward expansion of the low salinity waters of the warm pool, as suggested by some models (Delcroix and Picaut 1998), then changes in horizontal advection may have also significantly contributed to the observed freshening trend.

The magnitude of the late-twentieth-century $\delta^{18}O_{SW}$ trend is large relative to the natural decadal-scale $\delta^{18}O_{SW}$ variability contained in the coral record. The century-long $-0.25‰$ trend in $\delta^{18}O_{SW}$ amounts to a roughly -0.9 psu trend in salinity assuming the Fairbanks et al. (1997) empirical relationship between $\delta^{18}O_{SW}$ and salinity in the central tropical Pacific. Instrumental salinity data from the central tropical Pacific resolve a freshening trend on the order of -0.15 psu from 1970 to 2003 (Delcroix et al. 2007), which can be compared to the coral $\delta^{18}O_{SW}$-based freshening trend over the same time period. The Palmyra coral-based $\delta^{18}O_{SW}$ trend amounts to $-0.32‰$ from 1970 to 1998, or approximately -1.2 psu using the Fairbanks et al. empirical $\delta^{18}O_{SW}$–salinity relationship. The discrepancy between the instrumental and coral-based salinity trend estimates likely arises from large uncertainties associated with the empirical relationship between $\delta^{18}O_{SW}$ and salinity, which is poorly constrained by a sparse dataset of seawaters collected over a period of ~18 months (Fairbanks et al. 1997). However, large uncertainties in the instrumental salinity data assembled from scant ships of opportunity, moored ocean buoys, and isolated research cruises may also contribute to the discrepancy. If we scale the century-long coral $\delta^{18}O_{SW}$ trend to the late-twentieth-century Delcroix et al. (2007) sea surface salinity trend, we calculate a century-long freshening of -0.12 psu. Ultimately, the magnitude of coral $\delta^{18}O_{SW}$-derived salinity trends will remain highly uncertain until longer time series of paired seawater $\delta^{18}O_{SW}$ and sea surface salinity become available.

Within the context of the millennium-long coral $\delta^{18}O$ record (Cobb et al. 2003), the twentieth-century $\delta^{18}O_{SW}$-based salinity proxy record suggests that changes in the large-scale hydrological cycle associated with weakened

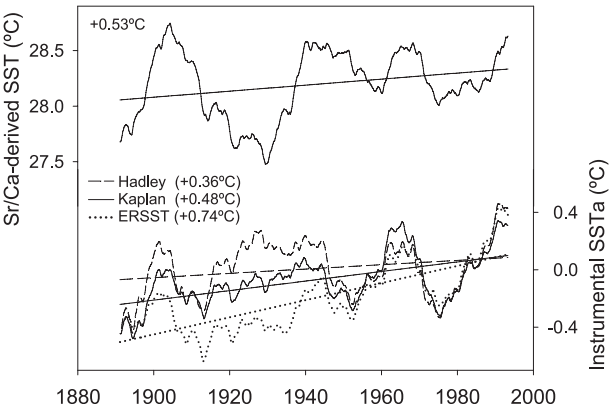

FIG. 8. Coral-based and instrumental SST trends at Palmyra over the twentieth century (1886–1998): 10-yr-averaged (top) coral Sr/Ca-derived SST with linear trend and (bottom) instrumental SST anomalies and linear trends from the Hadley (Rayner et al. 2006), Kaplan (Kaplan et al. 1998), and ERSST (Smith et al. 2008) datasets for the Palmyra grid point.

tropical circulation may dominate anthropogenic climate changes in the tropical Pacific. Indeed, the unprecedented trend toward lower coral $\delta^{18}O$ values during the late twentieth century observed in a millennium-long coral $\delta^{18}O$ reconstruction (Cobb et al. 2003; Fig. 1) can be entirely explained by the observed $\delta^{18}O_{SW}$ trend. Similar late-twentieth-century negative coral $\delta^{18}O$ trends have also been observed in other coral $\delta^{18}O$ records from the central and western tropical Pacific (Cole and Fairbanks 1990; Evans et al. 1999; Guilderson and Schrag 1999; Urban et al. 2000; Tudhope et al. 2001; Quinn et al. 2006) and from regions sensitive to South Pacific convergence zone (SPCZ) variability (Kilbourne et al. 2004; Linsley et al. 2006), consistent with widespread changes in the tropical Pacific hydrological cycle. Analyses of rain gauge data (Morrissey and Graham 1996), instrumental salinity datasets (Delcroix et al. 2007; Durack and Wijffels 2010), and coral-based $\delta^{18}O_{SW}$ salinity proxy records (Linsley et al. 2006; Nurhati et al. 2009) indicate freshening trends may be associated with enhanced precipitation in regions characterized by convective activity, consistent with enhanced hydrological patterns inferred from GCM simulations of twenty-first-century climate (Held and Soden 2006).

4. Conclusions

This study presents monthly resolved coral Sr/Ca-based SST and $\delta^{18}O_{SW}$-derived salinity proxy records from Palmyra Island, located in the central tropical Pacific, that span the twentieth century. The century-long coral SST proxy record is dominated by interannual and decadal-scale variations that are linked to central Pacific warming variability. Conversely, the coral-based $\delta^{18}O_{SW}$ salinity proxy record documents the influence of eastern Pacific ENSO and the PDO on tropical Pacific salinity variability and is dominated by a prominent freshening trend in the late twentieth century. That the freshening trend is likely unprecedented in the last millennium means that it is most likely associated with anthropogenic climate change. Taken together, the proxy records reveal that SST and precipitation variations are largely decoupled on interannual, decadal, and secular time scales and that anthropogenic hydrological trends may be more detectable than SST trends in the tropical Pacific. The records provide new insights into the mechanisms and impacts of low-frequency Pacific climate variability and, together with other such long, continuous coral climate reconstructions, may improve climate projections for regions that are heavily influenced by tropical Pacific climate variability.

Acknowledgments. The authors thank the Donors of the American Chemical Society-Petroleum Research Fund for funding the research as a grant to KMC; thanks are also extended for grants NSF OCE-0550266 and NSF GLOBEC OCE-0815280 to EDL. The authors thank Heather Crespo and Hussein Sayani for assistance with generating SEM images. The manuscript benefited greatly from the comments of Thierry Corrège as well as two anonymous reviewers.

APPENDIX

Error Propagation Analyses

a. Sr/Ca-derived SST (absolute SST)

The compounded error for any given absolute SST estimate in the coral Sr/Ca-based record (σ_{SST}) includes uncertainties associated with (i) the analytical precision of Sr/Ca measurements (σ_{SrCa}) and (ii) the intercept (σ_a) and (iii) the slope (σ_b) of the SST–Sr/Ca calibration. Starting with the equation for estimating SST from coral Sr/Ca and their associated errors,

$$\mathrm{SST} = a + b\mathrm{Sr/Ca} \tag{A1}$$

and

$$\mathrm{SST} \pm \sigma_{SST} = (a \pm \sigma_a) + (b \pm \sigma_b)(\overline{\mathrm{Sr/Ca}} + \sigma_{SrCa}). \tag{A2}$$

The last term, a multiplicative compounded error associated with the Sr/Ca–SSTcalibration slope and the analytical precision of Sr/Ca measurements, $[(b \pm \sigma_b)(\overline{\mathrm{Sr/Ca}} \pm \sigma_{SrCa})]$, is calculated via

$$\sigma_{\mathrm{slope_analytical}} = |b\overline{\mathrm{SrCa}}| \sqrt{(\sigma_b/b)^2 + (\sigma_{SrCa}/\overline{\mathrm{SrCa}})^2}. \tag{A3}$$

Thus, the compounded error for SST estimates by adding the calibration intercept error (σ_a) is

$$\sigma_{SST} = \sqrt{\sigma_a^2 + \sigma_{\mathrm{slope_analytical}}^2} \tag{A4}$$

and

$$\sigma_{SST} = \sqrt{\sigma_a^2 + (b\overline{\mathrm{SrCa}})^2[(\sigma_b/b)^2 + (\sigma_{SrCa}/\overline{\mathrm{SrCa}})^2]}. \tag{A5}$$

Substituting known values for each term and their uncertainties,

$$\mathrm{SST} \pm \sigma_{SST} = (130.43 \pm 5.54) + (-11.39 \pm 0.62) \times (8.98 \pm 0.006). \tag{A6}$$

The compounded error for SST estimates at Palmyra yields

$$\sigma_{SST} = \sqrt{5.54^2 + (-11.39 \times 8.98)^2 \times \left[\left(\frac{0.62}{-11.39}\right)^2 + \left(\frac{0.006}{8.98}\right)^2\right]} = 7.85°C. \quad \text{(A7)}$$

b. Sr/Ca-derived SST trend (relative SST changes)

When considering the errors associated with relative changes in coral Sr/Ca-based SST, a different set of calculations applies because some of the large uncertainties associated with the Sr/Ca–SST calibration have no impact on the calculation of relative SST changes. Uncertainty in the Sr/Ca-derived SST trend must take into account errors associated with (i) the slope error of the trend, (ii) the analytical precision of the Sr/Ca measurements via ICP-OES, and (iii) the calibration slope of the Sr/Ca–SST calibration (the intercept of the calibration would not affect the Sr/Ca-derived SST trend error). The details are as follow.

(i) The century-long Sr/Ca-derived SST trend is +0.53°C with a trend slope error of ±0.07°C (1σ).
(ii) The Sr/Ca-derived SST trend error associated with the analytical precision of coral Sr/Ca via ICP-OES is ±0.07°C (1σ), which represents the conservative assumption of applying the maximum error ranges of the analytical precision.
(iii) The calibration slopes and slope errors of the coral Sr/Ca –SST egression are −11.39 ± 0.62°C (mmol/mol)$^{-1}$ (1σ) at Palmyra. The uncertainty in coral Sr/Ca trends associated with calibration slope error is ±0.03°C (1σ), which is the difference between the SST trends calculated with maximum and minimum Sr/Ca–SST slopes (+0.50° and +0.56°C, respectively) from the original trend of +0.53°C at Palmyra.

Taken together, the twentieth-century Palmyra coral Sr/Ca-derived SST trend is 0.53 ± 0.10°C (1σ), quadratically combining terms (i)–(iii).

c. $\delta^{18}O_{SW}$-based salinity (absolute $\delta^{18}O_{SW}$)

As $\delta^{18}O_{SW}$ is calculated using relative changes in coral Sr/Ca-based SST, the record by definition represents relative changes in $\delta^{18}O_{SW}$. The choice of absolute value for the $\delta^{18}O_{SW}$ series is subject to large uncertainties, as it relies on an empirical relationship between salinity and $\delta^{18}O_{SW}$ obtained in the central tropical Pacific (Fairbanks et al. 1997). The compounded error for $\delta^{18}O_{SW}$ estimates includes uncertainties associated with analytical precisions of (i) coral $\delta^{18}O$ and (ii) Sr/Ca, as well as the slopes of (iii) coral $\delta^{18}O$-SST regression and (iv) Sr/Ca–SST calibration. Starting with the equation for calculating changes in $\delta^{18}O_{SW}$, which is sensitive to coral $\delta^{18}O$ and SST variability, and following the method of outlined in Ren et al. (2003):

$$\Delta\delta^{18}O_{CORAL} = \Delta\delta^{18}O_{SST} + \Delta\delta^{18}O_{SW} \quad \text{(A8)}$$

and

$$\Delta\delta^{18}O_{CORAL} \pm \sigma_{\Delta\delta^{18}O_{CORAL}} = (\Delta\delta^{18}O_{SST} \pm \sigma_{\Delta\delta^{18}O_{SST}}) + (\Delta\delta^{18}O_{SW} \pm \sigma_{\Delta\delta^{18}O_{SW}}) \quad \text{(A9)}$$

in which the delta symbol (Δ) refers to the difference between values from two adjacent months.

Taking the lhs of (A9) first, the equation for $\Delta\delta^{18}O_{CORAL}$ is

$$\Delta\delta^{18}O_{CORAL} = \delta^{18}O_{CORAL}(t) - \delta^{18}O_{CORAL}(t-1) \quad \text{(A10)}$$

and

$$\Delta\delta^{18}O_{CORAL} \pm \sigma_{\Delta\delta^{18}O_{CORAL}} = [\delta^{18}O_{CORAL}(t) \pm \sigma_{\delta^{18}O_{CORAL}}] - [\delta^{18}O_{CORAL}(t-1) \pm \sigma_{\delta^{18}O_{CORAL}}] \quad \text{(A11)}$$

Analytical error associated with the Cobb et al. (2001) coral $\delta^{18}O$ record was reported as ±0.05‰ (1σ; long-term $\delta^{18}O$ reproducibility). Thus, the calculation for the error associated with $\Delta\delta^{18}O_{CORAL}$ follows the equation

$$\sigma_{\Delta\delta^{18}O_{CORAL}} = \sqrt{\sigma^2_{\delta^{18}O_{CORAL}} + \sigma^2_{\delta^{18}O_{CORAL}}} = \sigma_{\delta^{18}O_{CORAL}}\sqrt{2} = 0.05\sqrt{2} = 0.07‰. \quad \text{(A12)}$$

Taking the first term on the rhs of (A9), the equation for $\Delta\delta^{18}O_{SST}$ is

$$\Delta\delta^{18}O_{SST} = \left[\overline{\Delta SrCa}\,\frac{\partial SST}{\partial SrCa}\,\frac{\partial\delta^{18}O_{CORAL}}{\partial SST}\right], \quad \text{(A13)}$$

where $\overline{\Delta SrCa}$ is the mean of the absolute values of ΔSrCa (because the ΔSrCa time series contains both positive and negative signs). The calculated value for $\overline{\Delta SrCa}$ is 0.03 mmol mol^{-1}, with an error bar of ±0.01 mmol mol^{-1}, considering the ±0.006 mmol mol^{-1} analytical precision of Sr/Ca measurements and following these calculations:

$$\Delta SrCa = SrCa(t) - SrCa(t-1) \quad \text{and} \quad \text{(A14)}$$

$$\Delta SrCa \pm \sigma_{\Delta SrCa} = [SrCa(t) \pm \sigma_{SrCa}] - [SrCa(t-1) \pm \sigma_{SrCa}], \quad \text{(A15)}$$

thus

$$\sigma_{\Delta SrCa} = \sqrt{\sigma_{SrCa}^2 + \sigma_{SrCa}^2} = \sigma_{SrCa}\sqrt{2} = 0.006\sqrt{2} = 0.01 \text{ mmol mol}^{-1}, \quad \text{(A16)}$$

where $\partial SST/\partial SrCa$ is the slope of the Sr/Ca–SST calibration, which is -11.39 ± 0.62°C (mmol/mol)$^{-1}$, and $\partial\delta^{18}O_{CORAL}/\partial SST$ of -0.21 ± 0.03‰°C^{-1} is the mean empirical values of coral $\delta^{18}O$ sensitivity to SST compiled by Ren et al. (2003).

The calculation for the error associated with $\Delta\delta^{18}O_{SST}$ following Eq. (A13) is

$$\sigma_{\Delta\delta^{18}O_{SST}} = \left|\overline{\Delta SrCa}\,\frac{\partial SST}{\partial SrCa}\,\frac{\partial\delta^{18}O_{CORAL}}{\partial SST}\right|\sqrt{\left(\frac{\sigma_{\Delta SrCa}}{\Delta SrCa}\right)^2 + \left(\frac{\sigma_{SST-SrCa\ Slope}}{SST-SrCa\ Slope}\right)^2 + \left(\frac{\sigma_{coral\ \delta^{18}O-SST_{Slope}}}{coral\ \delta^{18}O\ -\ SST_{Slope}}\right)^2}. \quad \text{(A17)}$$

Substituting in the known values yields

$$\sigma_{\Delta\delta^{18}O_{SST}} = |0.03(-11.39)(-0.21)|\sqrt{\left(\frac{0.01}{0.03}\right)^2 + \left(\frac{0.62}{-11.39}\right)^2 + \left(\frac{0.03}{-0.21}\right)^2} = 0.02‰. \quad \text{(A18)}$$

Having calculated $\Delta\delta^{18}O_{CORAL}$ and $\Delta\delta^{18}O_{SST}$, the compounded error for $\Delta\delta^{18}O_{SW}$ is calculated as the additive error propagation of the two terms:

$$\sigma_{\Delta\delta^{18}O_{SW}} = \sqrt{\sigma_{\Delta\delta^{18}O_{CORAL}}^2 + \sigma_{\Delta\delta^{18}O_{SST}}^2} = \sqrt{0.07^2 + 0.02^2} = 0.07‰. \quad \text{(A19)}$$

Since

$$\Delta\delta^{18}O_{SW} = \delta^{18}O_{SW}(t) - \delta^{18}O_{SW}(t-1) \quad \text{and} \quad \text{(A20)}$$

$$\Delta\delta^{18}O_{SW} \pm \sigma_{\Delta\delta^{18}O_{SW}} = [\delta^{18}O_{SW}(t) \pm \sigma_{\delta^{18}O_{SW}}] - [\delta^{18}O_{SW}(t-1) \pm \sigma_{\delta^{18}O_{SW}}] \quad \text{(A21)}$$

thus

$$\sigma_{\Delta\delta^{18}O_{SW}} = \sqrt{\sigma_{\delta^{18}O_{SW}}^2 + \sigma_{\delta^{18}O_{SW}}^2} = \sigma_{\delta^{18}O_{SW}}\sqrt{2}. \quad \text{(A22)}$$

Therefore, the compounded error for $\delta^{18}O_{SW}$ is

$$\sigma_{\delta^{18}O_{SW}} = \sigma_{\Delta\delta^{18}O_{SW}}\sqrt{2} = 0.07\sqrt{2} = 0.1‰ \quad \text{(A23)}$$

d. $\delta^{18}O_{SW}$-based salinity trend (relative $\delta^{18}O_{SW}$ changes)

The twentieth-century trend in Palmyra coral-based $\delta^{18}O_{SW}$ amounts to -0.25‰. There are five sources of uncertainty that contribute to uncertainties in this coral $\delta^{18}O_{SW}$ trend: (i) analytical precision of coral $\delta^{18}O$ via mass spectrometer, (ii) analytical precision of coral Sr/Ca via ICP-OES, (iii) slope error of the trend, (iv) slope error in the coral Sr/Ca–SST calibration, and (v) slope error in the coral $\delta^{18}O$–SST regression with the following details.

(i) The analytical precision associated with the Cobb et al. (2001) coral $\delta^{18}O$ record was reported as ± 0.05‰ (1σ, long-term $\delta^{18}O$ reproducibility).
(ii) The analytical precision of coral Sr/Ca via ICP-OES of ± 0.07°C (1σ) translates to a ± 0.01‰ (1σ) $\delta^{18}O_{SW}$ trend error via the empirical mean $\delta^{18}O$–SST slope regression of -0.21‰ °C^{-1} (Ren et al. 2003).
(iii) The fitting of a trend line on coral-based $\delta^{18}O_{SW}$ records has slope errors of ± 0.01‰ at Palmyra.
(iv) The calibration slopes and slope errors of the coral Sr/Ca–SST regression is -11.39 ± 0.62°C (mmol/mol)$^{-1}$ (1σ) at Palmyra. This would yield an uncertainty in $\delta^{18}O_{SW}$ trends of ± 0.01‰ (1σ), which is the difference between the minimum and maximum trends calculated with analytical error (-0.24‰ and -0.26‰, respectively) from the original trend of -0.25‰ at Palmyra.
(v) The empirical slope for coral $\delta^{18}O$–SST regression is -0.21 ± 0.03‰ °C^{-1} following values compiled by Ren et al. (2003). This would yield an uncertainty in $\delta^{18}O_{SW}$ trends of ± 0.02‰ (1σ), which is the difference between the minimum and maximum trends (-0.23‰ and -0.27‰, respectively) calculated with minimum and maximum $\delta^{18}O$–SST, from the original trend of -0.25‰ at Palmyra.

Taken together, the twentieth-century Palmyra coral-based $\delta^{18}O_{SW}$ trend and its associated uncertainty is

$-0.25 \pm 0.06‰$ (1σ), quadratically combining terms (i)–(v) above.

REFERENCES

Alexander, M. A., I. Bladé, M. Newman, J. R. Lanzante, N. C. Lau, and J. D. Scott, 2002: The atmospheric bridge: The influence of ENSO teleconnections on air–sea interaction over the global oceans. *J. Climate,* **15,** 2205–2231.

——, N.-C. Lau, and J. D. Scott, 2004: Broadening the atmospheric bridge paradigm: ENSO teleconnections to the North Pacific in summer and to the tropical west Pacific-Indian Oceans over the seasonal cycle. *Earth Climate: The Ocean–Atmosphere Interaction, Geophys. Monogr.,* Vol. 147, Amer. Geophys. Union, 85–104.

Alibert, C., and M. T. McCulloch, 1997: Strontium/calcium ratios in modern Porites corals from the Great Barrier Reef as a proxy for sea surface temperature: Calibration of the thermometer and monitoring of ENSO. *Paleoceanography,* **12,** 345–363, doi:10.1029/97PA00318.

Ashok, K., S. K. Behera, S. A. Rao, H. Weng, and T. Yamagata, 2007: El Niño Modoki and its possible teleconnection. *J. Geophys. Res.,* **112,** C11007, doi:10.1029/2006JC003798.

Ault, T. R., J. E. Cole, M. N. Evans, H. Barnett, N. J. Abram, A. W. Tudhope, and B. K. Linsley, 2009: Intensified decadal variability in tropical climate during the late 19th century. *Geophys. Res. Lett.,* **36,** L08602, doi:10.1029/2008GL036924.

Beck, J. W., R. L. Edwards, E. Ito, F. W. Taylor, J. Recy, F. Rougerie, P. Joannot, and C. Henin, 1992: Sea-surface temperature from coral skeletal strontium/calcium ratios. *Science,* **257,** 644–647, doi:10.1126/science.257.5070.644.

Bretherton, C. S., M. Widmann, V. P. Dymnikov, J. M. Wallace, and I. Bladé, 1999: Effective number of degrees of freedom of a spatial field. *J. Climate,* **12,** 1990–2009.

Bunge, L., and A. J. Clarke, 2009: A verified estimation of the El Niño index Niño-3.4 since 1877. *J. Climate,* **22,** 3979–3992.

Chen, G., and C.-Y. Tam, 2010: Different impacts of two kinds of Pacific Ocean warming on tropical cyclone frequency over the western North Pacific. *Geophys. Res. Lett.,* **37,** L01803, doi:10.1029/2009GL041708.

Cobb, K. M., C. D. Charles, and D. E. A. Hunter, 2001: A central tropical Pacific coral demonstrates Pacific, Indian, and Atlantic decadal climate connections. *Geophys. Res. Lett.,* **28,** 2209–2212, doi:10.1029/2001GL012919.

——, ——, H. Cheng, and R. L. Edwards, 2003: El Niño/Southern Oscillation and tropical Pacific climate during the last millennium. *Nature,* **424,** 271–276, doi:10.1038/nature01779.

Cole, J. E., and R. G. Fairbanks, 1990: The Southern Oscillation recorded in the $\delta^{18}O$ of corals from Tarawa Atoll. *Paleoceanography,* **5,** 669–683, doi:10.1029/PA005i005p00669.

——, ——, and G. T. Shen, 1993: Recent variability in the Southern Oscillation: Isotopic results from a Tarawa Atoll coral. *Science,* **260,** 1790–1793, doi:10.1126/science.260.5115.1790.

Corrège, T., 2006: Sea surface temperature and salinity reconstruction from coral geochemical tracers. *Palaeogeogr. Palaeoclimatol. Palaeoecol.,* **232,** 408–428, doi:10.1016/j.palaeo.2005.10.014.

Delcroix, T., and J. Picaut, 1998: Zonal displacement of the western equatorial Pacific "fresh pool." *J. Geophys. Res.,* **103,** 1087–1098, doi:10.1029/97JC01912.

——, S. Cravatte, and M. J. McPhaden, 2007: Decadal variations and trends in tropical Pacific sea surface salinity since 1970. *J. Geophys. Res.,* **112,** C03012, doi:10.1029/2006JC003801.

Deser, C., A. S. Phillips, and J. W. Hurrell, 2004: Pacific interdecadal climate variability: Linkages between the tropics and the North Pacific during boreal winter since 1900. *J. Climate,* **17,** 3109–3124.

——, M. A. Alexander, S.-P. Xie, and A. S. Phillips, 2010: Sea surface temperature variability: Patterns and mechanisms. *Annu. Rev. Mar. Sci.,* **2,** 115–143, doi:10.1146/annurev-marine-120408-151453.

Di Lorenzo, E., and Coauthors, 2008: North Pacific gyre oscillation links ocean climate and ecosystem change. *Geophys. Res. Lett.,* **35,** L08607, doi:10.1029/2007GL032838.

——, K. M. Cobb, J. C. Furtado, N. Schneider, B. Anderson, A. Bracco, M. A. Alexander, and D. Vimont, 2010: Central Pacific El Niño and decadal climate change in the North Pacific. *Nat. Geosci.,* **3,** 762–765, doi:10.1038/NGEO984.

DiNezio, P. N., A. C. Clement, G. A. Vecchi, B. J. Soden, B. P. Kirtman, and S. K. Lee, 2009: Climate response of the equatorial Pacific to global warming. *J. Climate,* **22,** 4873–4892.

Durack, P. J., and S. E. Wijffels, 2010: Fifty-year trends in global ocean salinities and their relationship to broad-scale warming. *J. Climate,* **23,** 4342–4362.

Enmar, R., M. Stein, M. Bar-Matthews, E. Sass, A. Katz, and B. Lazar, 2000: Diagenesis in live corals from the Gulf of Aqaba. I. The effect on paleo-oceanography tracers. *Geochim. Cosmochim. Acta,* **64,** 3123–3132, doi:10.1016/S0016-7037(00)00417-8.

Evans, M. N., R. G. Fairbanks, and J. L. Rubenstone, 1999: The thermal oceanographic signal of El Niño reconstructed from a Kiritimati Island coral. *J. Geophys. Res.,* **104,** 13 409–13 421, doi:10.1029/1999JC900001.

——, A. Kaplan, and M. A. Cane, 2002: Pacific sea surface temperature field reconstruction from coral $\delta^{18}O$ data using reduced space objective analysis. *Paleoceanography,* **17,** 1007, doi:10.1029/2000PA000590.

Fairbanks, R. G., M. N. Evans, J. L. Rubenstone, R. A. Mortlock, K. Broad, M. D. Moore, and C. D. Charles, 1997: Evaluating climate indices and their geochemical proxies measured in corals. *Coral Reefs,* **16,** S93–S100, doi:10.1007/s003380050245.

Gagan, M. K., L. K. Ayliffe, D. Hopley, J. A. Cali, G. E. Mortimer, J. Chappell, M. T. McCulloch, and M. J. Head, 1998: Temperature and surface-ocean water balance of the mid-Holocene tropical western Pacific. *Science,* **279,** 1014–1018, doi:10.1126/science.279.5353.1014.

——, ——, J. W. Beck, J. E. Cole, E. M. Druffel, R. B. Dunbar, and D. P. Schrag, 2000: New views of tropical paleoclimates from corals. *Quat. Sci. Rev.,* **19,** 45–64, doi:10.1016/S0277-3791(99)00054-2.

Guilderson, T. P., and D. P. Schrag, 1999: Reliability of coral isotope records from the western Pacific warm pool: A comparison using age-optimized records. *Paleoceanography,* **14,** 457–464, doi:10.1029/1999PA900024.

Held, I. M., and B. J. Soden, 2006: Robust responses of the hydrological cycle to global warming. *J. Climate,* **19,** 5686–5699.

Hendy, E. J., M. K. Gagan, C. A. Alibert, M. T. McCulloch, J. M. Lough, and P. J. Isdale, 2002: Abrupt decrease in tropical Pacific sea surface salinity at end of Little Ice Age. *Science,* **295,** 1511–1514, doi:10.1126/science.1067693.

——, ——, J. M. Lough, M. McCulloch, and P. B. deMenocal, 2007: Impact of skeletal dissolution and secondary aragonite on trace element and isotopic climate proxies in Porites corals. *Paleoceanography,* **22,** PA4101, doi:10.1029/2007pa001462.

Holland, C. L., R. B. Scott, S. I. An, and F. W. Taylor, 2007: Propagating decadal sea surface temperature signal identified in modern proxy records of the tropical Pacific. *Climate Dyn.,* **28,** 163–179, doi:10.1007/s00382-006-0174-0.

Kao, H.-Y., and J.-Y. Yu, 2009: Contrasting eastern Pacific and central Pacific types of ENSO. *J. Climate,* **22,** 615–632.

Kaplan, A., M. Cane, Y. Kushnir, A. Clement, M. Blumenthal, and B. Rajagopalan, 1998: Analyses of global sea surface temperature 1856–1991. *J. Geophys. Res.,* **103,** 18 567–18 589, doi:10.1029/97JC01736.

Kilbourne, K. H., T. M. Quinn, F. W. Taylor, T. Delcroix, and Y. Gouriou Y, 2004: El Niño–Southern Oscillation-related salinity variations recorded in the skeletal geochemistry of a *Porites* coral from Espiritu Santo, Vanuatu. *Paleoceanography,* **19,** PA4002, doi:10.1029/2004PA001033.

Kim, H.-M., P. J. Webster, and J. A. Curry, 2009: Impact of shifting patterns of Pacific Ocean warming on North Atlantic tropical cyclones. *Science,* **325,** 77–80, doi:10.1126/science.1174062.

Kug, J.-S., F.-F. Jin, and S.-I. An, 2009: Two types of El Niño events: Cold tongue El Niño and warm pool El Niño. *J. Climate,* **22,** 1499–1515.

Kumar, K. K., B. Rajagopalan, M. Hoerling, G. Bates, and M. Cane, 2006: Unraveling the mystery of Indian monsoon failure during El Niño events. *Science,* **314,** 115–119, doi:10.1126/science.1131152.

Larkin, N. K., and D. E. Harrison, 2005: Global seasonal temperature and precipitation anomalies during El Niño autumn and winter. *Geophys. Res. Lett.,* **32,** L13705, doi:10.1029/2005GL022738.

Latif, M., R. Kleeman, and C. Eckert, 1997: Greenhouse warming, decadal variability, or El Niño? An attempt to understand the anomalous 1990s. *J. Climate,* **10,** 2221–2239.

Levitus, S., R. Burgett, and T. P. Boyer, 1994: *Salinity*. Vol. 3, *World Ocean Atlas 1994,* NOAA Atlas NESDIS 3, 99 pp.

Linsley, B. K., A. Kaplan, Y. Gouriou, J. Salinger, P. B. deMenocal, G. M. Wellington, and S. S. Howe, 2006: Tracking the extent of the South Pacific Convergence Zone since the early 1600s. *Geochem. Geophys. Geosyst.,* **7,** Q05003, doi:10.1029/2005GC001115.

Liu, Z., S. J. Vavrus, F. He, N. Wen, and Y. Zhang, 2006: Rethinking tropical ocean response to global warming: The enhanced equatorial warming. *J. Climate,* **18,** 4684–4700.

Mantua, N. J., S. R. Hare, Y. Zhang, J. M. Wallace, and R. C. Francis, 1997: A Pacific interdecadal climate oscillation with impacts on salmon production. *Bull. Amer. Meteor. Soc.,* **78,** 1069–1079.

McCulloch, M. T., M. K. Gagan, G. E. Mortimer, A. R. Chivas, and P. J. Isdale, 1994: A high resolution Sr/Ca and δ^{18}O coral record from the Great Barrier Reef, Australia, and the 1982–1983 El Niño. *Geochim. Cosmochim. Acta,* **58,** 2747–2754, doi:10.1016/0016-7037(94)90142-2.

McPhaden, M. J., and Coauthors, 1998: The Tropical Ocean-Global Atmosphere observing system: A decade of progress. *J. Geophys. Res.,* **103,** 14 169–14 240, doi:10.1029/97JC02906.

Meehl, G. A., and Coauthors, 2007: Global climate projections. *Climate Change 2007: The Physical Science Basis,* S. Solomon et al., Eds., Cambridge University Press, 747–846.

Morrissey, M. L., and N. E. Graham, 1996: Recent trends in rain gauge precipitation measurements from the tropical Pacific: Evidence for an enhanced hydrologic cycle. *Bull. Amer. Meteor. Soc.,* **77,** 1207–1219.

Newman, M., G. P. Compo, and M. A. Alexander, 2003: ENSO-forced variability of the Pacific decadal oscillation. *J. Climate,* **16,** 3853–3857.

Nurhati, I. S., K. M. Cobb, C. D. Charles, and R. B. Dunbar, 2009: Late 20th century warming and freshening in the central tropical Pacific. *Geophys. Res. Lett.,* **36,** L21606, doi:10.1029/2009GL040270.

Picaut, J., M. Ioualalen, C. Menkes, T. Delcroix, and M. J. McPhaden, 1996: Mechanism of the zonal displacements of the Pacific warm pool: Implications for ENSO. *Science,* **274,** 1486–1489, doi:10.1126/science.274.5292.1486.

Pierce, D. W., 2002: The role of sea surface temperatures in interactions between ENSO and the North Pacific Oscillation. *J. Climate,* **15,** 1295–1308.

Quinn, T. M., and F. W. Taylor, 2006: SST artifacts in coral proxy records produced by early marine diagenesis in a modern coral from Rabaul, Papua New Guinea. *Geophys. Res. Lett.,* **33,** L04601, doi:10.1029/2005GL024972.

——, ——, and T. J. Crowley, 2006: Coral-based climate variability in the western Pacific warm pool since 1867. *J. Geophys. Res.,* **111,** C11006, doi:10.1029/2005JC003243.

Rasmusson, E. M., and T. H. Carpenter, 1982: Variation in tropical sea surface temperature and surface wind fields associated with Southern Oscillation/El Niño. *Mon. Wea. Rev.,* **110,** 354–384.

Rayner, N. A., and Coauthors, 2006: Improved analyses of changes and uncertainties in sea surface temperature measured in situ since the mid-nineteenth century: The HadSST2 dataset. *J. Climate,* **19,** 446–469.

Ren, L., B. K. Linsley, G. M. Wellington, D. P. Schrag, and O. Hoegh-Guldberg, 2003: Deconvolving the δ^{18}O seawater component from subseasonal coral δ^{18}O and Sr/Ca at Rarotonga in the southwestern subtropical Pacific for the period 1726 to 1997. *Geochim. Cosmochim. Acta,* **67,** 1609–1621, doi:10.1016/S0016-7037(02)00917-1.

Reynolds, R. W., N. A. Rayner, T. M. Smith, D. C. Stokes, and W. Wang, 2002: An improved in situ and satellite SST analysis for climate. *J. Climate,* **15,** 1609–1625.

——, T. M. Smith, C. Liu, D. B. Chelton, K. S. Casey, and M. G. Schlax, 2007: Daily high-resolution-blended analyses for sea surface temperature. *J. Climate,* **20,** 5473–5496.

Schneider, N., and B. D. Cornuelle, 2005: The forcing of the Pacific decadal oscillation. *J. Climate,* **18,** 4355–4373.

Schrag, D. P., 1999: Rapid analysis of high-precision Sr/Ca ratios in corals and other marine carbonates. *Paleoceanography,* **14,** 97–102, doi:10.1029/1998PA900025.

Smith, T. M., R. W. Reynolds, T. C. Peterson, and J. Lawrimore, 2008: Improvements to NOAA's historical merged land–ocean surface temperature analysis (1880–2006). *J. Climate,* **21,** 2283–2296.

Solomon, S., D. Qin, M. Manning, M. Marquis, K. Averyt, M. M. B. Tignor, H. L. Miller Jr., and Z. Chen, Eds., 2007: *Climate Change 2007: The Physical Science Basis*. Cambridge University Press, 996 pp.

Solow, A. R., and A. Huppert, 2004: A potential bias in coral reconstruction of sea-surface temperature. *Geophys. Res. Lett.,* **31,** L06308, doi:10.1029/2003GL019349.

Trenberth, K. E., and D. P. Stepaniak, 2001: Indices of El Niño evolution. *J. Climate,* **14,** 1697–1701.

Tudhope, A. W., and Coauthors, 2001: Variability in the El Niño–Southern Oscillation through a glacial–interglacial cycle. *Science,* **291,** 1511–1517, doi:10.1126/science.1057969.

Urban, F. E., J. E. Cole, and J. T. Overpeck, 2000: Influence of mean climate change on climate variability from a 155-year tropical Pacific coral record. *Nature,* **407,** 989–993, doi:10.1038/35039597.

Vecchi, G. A., B. J. Soden, A. T. Wittenberg, I. M. Held, A. Leetmaa, and M. J. Harrison, 2006: Weakening of tropical Pacific

atmospheric circulation due to anthropogenic forcing. *Nature,* **441,** 73–76, doi:10.1038/nature04744.

——, A. Clement, and B. J. Soden, 2008: Examining the tropical Pacific's response to global warming. *Eos, Trans. Amer. Geophys. Union,* **89,** 81–83, doi:10.1029/2008EO090002.

Wang, G., and H. H. Hendon, 2007: Sensitivity of Australian rainfall to inter–El Niño variations. *J. Climate,* **20,** 4211–4226.

Weare, B. C., A. R. Navato, and R. E. Newell, 1976: Empirical orthogonal analysis of Pacific sea surface temperatures. *J. Phys. Oceanogr.,* **6,** 671–678.

Weng, H., S. K. Behera, and T. Yamagata, 2009: Anomalous winter climate conditions in the Pacific Rim during recent El Niño Modoki and El Niño events. *Climate Dyn.,* **32,** 663–674, doi:10.1007/s00382-008-0394-6.

Wyrtki, K., 1981: An estimate of equatorial upwelling in the Pacific. *J. Phys. Oceanogr.,* **11,** 1205–1214.

Xie, P., and P. A. Arkin, 1997: Global precipitation: A 17-year monthly analysis based on gauge observations, satellite estimates, and numerical model outputs. *Bull. Amer. Meteor. Soc.,* **78,** 2539–2558.

Xie, S. P., C. Deser, G. A. Vecchi, J. Ma, H. Teng, and A. T. Wittenberg, 2010: Global warming pattern formation: Sea surface temperature and rainfall. *J. Climate,* **23,** 966–986.

Yeh, S. W., J. S. Kug, B. Dewitte, M. H. Kwon, B. P. Kirtman, and F. F. Jin, 2009: El Niño in a changing climate. *Nature,* **461,** 511–514, doi:10.1038/nature08316.

Zhang, Y., J. M. Wallace, and D. S. Battisti, 1997: ENSO-like interdecadal variability: 1900–93. *J. Climate,* **10,** 1004–1020.